Cell J
Cell Journal(Yakhteh)
Homepage: https://www.celljournal.org/
Original Article
Vol 25, No 10, October 2023, Pages: 688-695

Role of The circ-HIPK3, circ-PVT1, miR-25, and miR-149 in Response of Breast Cancer Cells to Ionizing Radiation

Elahe Abdollahi, Ph.D.[1], Hossein Mozdarani, Ph.D.[1*]

Department of Medical Genetics, Faculty of Medical Sciences, Tarbiat Modares University, Tehran, Iran

Abstract

Objective: Determining cellular radiosensitivity of breast cancer (BC) patients through molecular markers before radiation therapy (RT) allows accurate prediction of individual's response to radiation. The aim of this study was therefore to investigate the potential role of epigenetic biomarkers in breast cancer cellular radiosensitivity.

Materials and Methods: In this experimental study, we treated two BC cell lines, MDA-MB 231 and MCF-7, with doses of 2, 4, and 8Gy of irradiation for 24 and 48 hours. Expression levels of circ-HIPK3, circ-PVT1, miR-25, and miR-149 were quantified using quantitative reverse-transcription polymerase chain reaction (qRT-PCR). Significance of the observations was statistically verified using one-way ANOVA with a significance level of $P<0.05$. Annexin V-FITC/PI binding assay was utilized to measure cellular apoptosis.

Results: The rate of cell apoptosis was significantly higher in MCF-7 cells compared to MDA-MB-231 cells at doses of 4Gy and 8Gy ($P=0.013$ and $P=0.004$, respectively). RNA expression analysis showed that circ-HIPK3 was increased in the MDA-MB-231 cell line compared to the MCF-7 cell line after exposure to 8Gy for 48 hours. Expression of circ-PVT1 was found to be higher in MDA-MB-231 cells compared to MCF-7 cells after exposure to 8Gy for 24 hours, likewise after exposure to 4Gy and 8Gy for 48 hours. After exposing 8Gy, expression of miR-25 was increased in MDA-MB-231 cells compared to MCF-7 cells at 24 and 48 hours. After exposing 8Gy dose, expression of miR-149 was increased in MCF-7 cells compared to MDA-MB-231 cells at 24 and 48 hours.

Conclusion: circ-HIPK3, circ-PVT1, and miR-25 played crucial roles in the mechanisms of radioresistance in breast cancer. Additionally, miR-149 was involved in regulating cellular radiosensitivity. Therefore, these factors provided predictive information about a tumor's radiosensitivity or its response to treatment, which could be valuable in personalizing radiation dosage.

Keywords: Breast Cancer, Ionizing Radiation, miR-149, miR-25

Citation: **Abdollahi E, Mozdarani H. Role of the circ-HIPK3, circ-PVT1, miR-25, and miR-149 in response of breast cancer cells to ionizing radiation. Cell J. 2023; 25(10): 688-695. doi: 10.22074/CELLJ.2023.1995943.1255**

Introduction

Breast cancer (BC) is the most diagnosed cancer among women globally and the primary cause of cancer-related fatalities in women (1). Radiation therapy (RT) is a common treatment used in approximately 50% of all cancer patients at some stage of their disease, as adjuvant therapy (2, 3). Ionizing radiation (IR) used in RT induces various types of DNA damage, including double-strand breaks (DSBs). DNA damage response (DDR) plays an important role in DSB repair and maintains genomic stability by protecting cells from apoptosis and malignancies (4). Levels of apoptosis are closely associated with cellular responses to IR. RNA expression can be involved in the epigenetic regulation of apoptosis (5). Circular RNAs (circRNAs) are a novel class of endogenous non-coding RNAs (ncRNAs) characterized by a closed-loop structure, which makes them resistant to degradation by RNases (6). This highlights the advantages of circRNA as a stable molecular biomarker for various types of cancer (7-12). circRNAs regulate expression of the related genes by specifically binding to microRNAs (miRNAs) and functioning as a sponge for them (13), thereby modulating expression of the target genes. miRNAs are a subtype of small non-coding RNA molecules, typically 20-25 nucleotides in length. They have been identified for their role in breast tumor development and regulation of radiation responses (7). miRNAs can influence tumor radiosensitivity through regulation of DDR (10).

Circular RNA homeodomain-interacting protein kinase 3 (circ-HIPK3 or hsa_circ_0000284) is produced through exon two back-splicing of the *HIPK3* gene located on chromosome 11 (14). Several studies showed that circ-HIPK3 was involved in progression of various types of cancer, including colorectal (15), glioblastoma (16), prostate (17), and breast cancers (18). High levels of

Received: 14/March/2023, Revised: 18/June/2023, Accepted: 16/July/2023
***Corresponding Address: P.O.Box: 14115-111, Department of Medical Genetics, Faculty of Medical Sciences, Tarbiat Modares University, Tehran, Iran**
Email: mozdarah@modares.ac.ir

Royan Institute
Cell Journal (Yakhteh)

circ-HIPK3 have been demonstrated in breast cancer; however, its expression was decreased when cancer cells underwent apoptosis. Overexpression of circ-HIPK3 has been shown to inhibit cell apoptosis in non-small-cell lung cancer (19), colorectal cancer (20), and BC (18). On the other hand, circRNA plasmacytoma variant translocation 1 (circ-PVT1 or hsa-circ-0001821) is a circRNAs molecule, originated from the *PVT1* gene, which is located on chromosome eight. This circRNA is formed through a process called exon two back-splicing. For convenience, this circRNA is referred to as circ-PVT1. Suppression of circ-PVT1 has been shown to promote BC cell apoptosis, while inhibiting proliferation, invasiveness, and migratory capacity (21).

Studies showed that circ-HIPK3 functioned as a miR-149 sponge, regulating activity of cancerous cells by controlling FOXM1 expression through miR-149-mediated regulation (19). circ-PVT1 enhanced FOXM1 expression by binding to miR-149-5p, thereby influencing the viability and migration of ovarian cancer cells (22). miR-149 is positively correlated with radiosensitivity in colorectal cancer (23).

Additionally, BC patients, who exhibited low serum miR-25-3p expression, had a higher overall survival rate compared to those with high serum miR-25-3p expression (24, 25). miR-25 has been identified as a contributing factor to radiosensitivity in lung cancer and therefore, it may serve as a potential target for enhancing effectiveness of the RT (25).

Using molecular markers can predict an individual's response to radiation and provide valuable insights into tumor sensitivity to radiation, as well as its potential response to treatment. This approach could be advantageous for customizing radiation dosage to optimize treatment outcomes. This would allow medical professionals to choose various treatment options, while reducing radiation-related harm in patients who are unlikely to benefit from treatment. For this purpose, we investigated potential involvement of these RNAs in response to the radiation and rates of apoptosis in BC cell lines. For the first time, we assessed expression levels of miR-149, miR-25, circ-PVT1, and circ-HIPK3 in two cell lines -one of which was resistant to radiation and the other one was sensitive to radiation. Finally, both cell lines were evaluated for apoptosis before and after irradiation.

Materials and Methods

This experimental study was conducted by ethical guidelines for laboratory cell line research and received approval from the Ethics Committee of the Research Department at Tarbiat Modares University in Tehran, Iran, ensuring compliance with ethical standards (IR.MODARES.REC.1400.176).

Cell culture

The MCF-7 and MDA-MB 231 human BC cells were obtained from the Pasteur Institute cell bank in Tehran, Iran. The cells were thawed from liquid nitrogen, washed, and cultured at a density of 1×10^6 cells per well in 6-well plates using Dulbecco's Modified Eagle medium (DMEM-F12) supplemented with 10% fetal bovine serum (FBS, Gibco, USA), penicillin, streptomycin, and glutamine (all from Gibco, USA). The cells were incubated at 37°C in a humidified atmosphere containing 5% CO_2.

Cell irradiation

The experiments were conducted at the Cancer Radiotherapy department in Pars Hospital (Tehran, Iran) using a Siemens Artiste linac that emitted 6 MV and 15 MV X-ray beams. Ten minutes before irradiation, the medium was replaced with a fresh complete medium to ensure proper backscatter. The cells were exposed to 6 MV and 15 MV photon radiation using a polystyrene phantom measuring $25\times25\times15$ cm³. The film exposures were performed using an open field size of 10×10 cm² at a depth of 5 cm. Two EBT3 films were used for each radiation beam. Each sheet was then cut into nine pieces with 6.8×8.5 cm² size. Therefore two films (one for each absorbed dose) were exposed to each X-ray at three dose levels: 2 Gy, 4 Gy, and 8 Gy. The other four films were considered zero-dose exposures.

Apoptosis detection by Annexin V-FITC/PI binding assay

Both cell lines (MDA-MB-231 and MCF-7 cells) were incubated for 24 and 48 hours after irradiation. Apoptotic cells were identified using the Annexin V-FITC Apoptosis Detection Kit from Sigma-Aldrich (USA). The target cells were detached using EDTA-free trypsin. To neutralize trypsin, serum containing DMEM (Gibco, USA) was used. The cells were then washed with 500 µl of flow buffer. After washing, 5 µl of fluorescein isothiocyanate (FITC)-labeled annexin V and 5 µl of propidium iodide (PI) were added to the tube containing the target cells. The mixture was then incubated at room temperature in dark for 15 minutes. Finally, cell apoptosis was measured using a BD FACSCalibur™ flow cytometer (BD Biosciences, USA) equipped with a fluorescence-activated cell sorter (FACS). Flowing software version 2.5.1 was used for data analysis.

Target selection

In this study, we investigated expression levels of hsa-miR-149, hsa-miR-25, circ-PVT1, and circ-HIPK3 in BC cell lines, as potential biomarkers for predicting radiosensitivity and radiotoxicity in BC patients undergoing radiotherapy. When selecting these non-coding RNAs, we had to consider various criteria, including their involvement in carcinogenesis and radio-responsiveness, as well as their expression in blood, rather than being tissue-specific. Furthermore, these miRNAs and circRNAs functioned within the same pathway and

exhibited interrelatedness. Based on these criteria, we selected RNAs that had previously been studied primarily in the cell lines and cancers other than BC, and that met all of the above criteria.

Designing primers

A stem-loop primer was designed for the reverse transcription of miRNAs. The primer sequences for the stem-loop used in this study are listed below:

hsa-miR-149:

5′-GTCGTACCAGTGCAGGGTCCCGA-3′
GGTATTCGCACTGGATACGACGGGAGT-3′

hsa-miR-25:

5′-GTCGTATCCAGTGCAGGGTCCGAGGTATTCG-CACTGGATACGACTCAGAC-3′

miRNA sequences were obtained from the miRBase database, and the primers were designed using the stem-loop method.

circRNA sequence was obtained from the circBase database. The junction region was identified using the circRNA Interactome database (Fig.1A, B), and primers were designed using divergent methods for both sides of the junction.

All primers were designed using the Primer3 database and validated using the Primer-BLAST tool. The primers list is presented in Table 1.

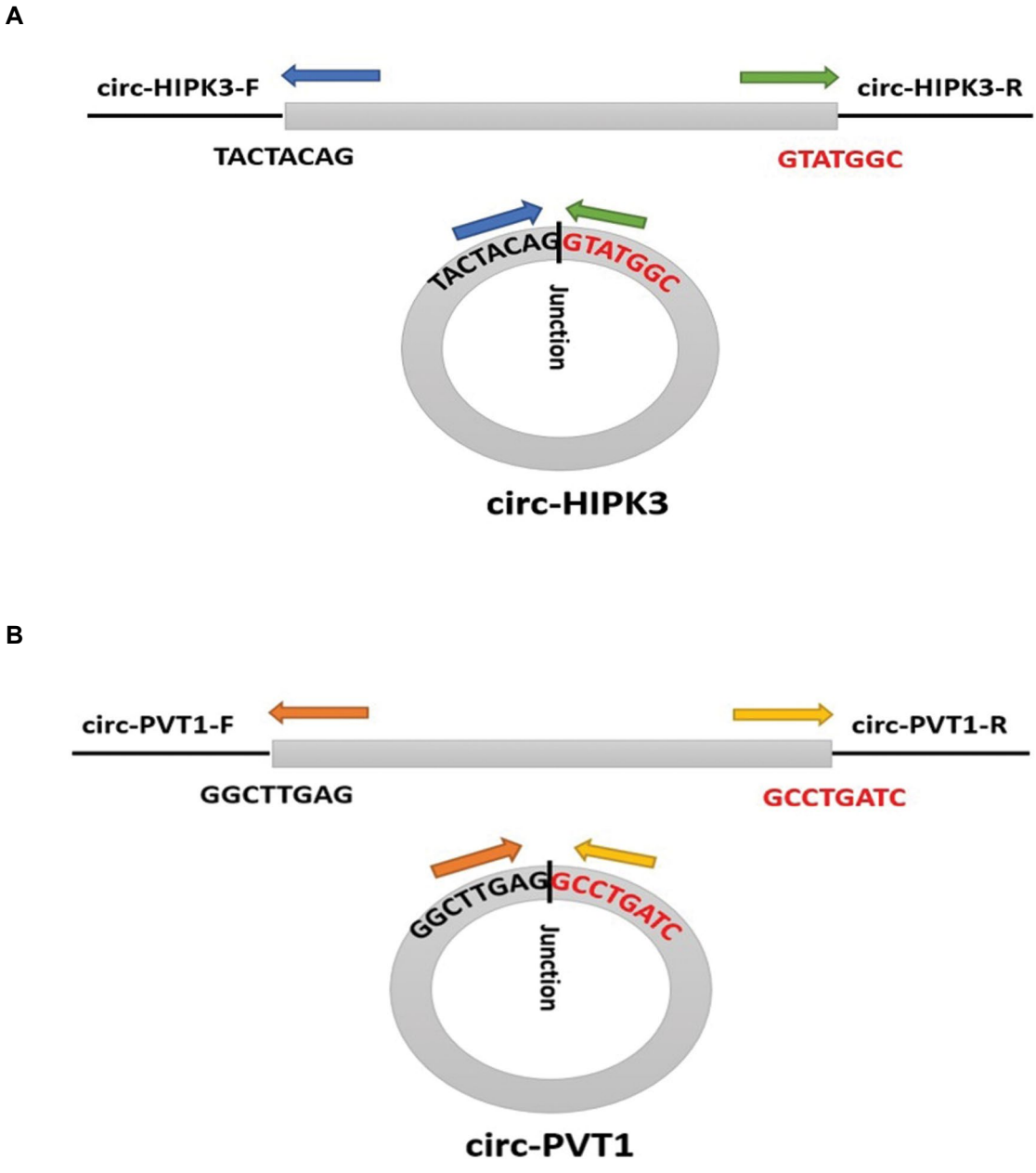

Fig.1: Scheme illustrating the production of circular RNAs and sequencing analysis of back-splicing junctions. **A.** circ-HIPK3 and **B.** circ-PVT1.

Table 1: Primer sequences utilized for quantitative reverse transcription polymerase chain reaction (qRT-PCR)

Target	Primer sequence (5′-3′)
circ-HIPK3	F: GGTCGGCCAGTCATGTATC
	R: ACTGCTTGGCTCTACTTTGAG
circ-PVT1	F: CTGCCAACTTCCTTTGGGTC
	R: AGGCACAGCCATCTTGAGG
miR-25	F: ACGATCTTTGCTCTTGTCTCG
	R: AATACCTCGGACCCTGCAC
miR-149	F: ACATCTGGCTCCGTGTCTTC
	R: AATACCTCGGACCCTGCAC
U6	F: CTCGCTTCGGCAGCACA
	R: AACGCTTCACGAATTTGCGT
GAPDH	F: ATGAGAAGTATGACAACAGCCTC
	R: CATGAGTCCTTCCACGATACC

RNA isolation and quantitative reverse transcription polymerase chain reaction

Total RNA was extracted from the cell lines using and TRIzol reagent (Invitrogen, Germany) following to the manufacturer's instructions. Purity and concentration of the RNA samples were determined using a NanoDrop ND-1000 spectrophotometer (Thermo Fisher Scientific, USA). For validation experiments, RNA was prepared and stored at -80°C. For cDNA synthesis, we utilized the qPCRBIO cDNA synthesis kit (PCR Biosystems Ltd., UK) and followed the manufacturer's protocol.

The reagents were gently mixed on ice. The reagents included miRNA, Stem-Loop RT primer (1 pM), and water. The mixture was then incubated at 70°C for five minutes. A mixture was prepared containing 5x first strand buffer, dNTP (10 mM each), and RNasin (40 units of MLV). The mixture was added to a tube and incubated at 16°C for 30 minutes and then at 60°C for 42 minutes using a PCR system (Eppendorf, Germany). The reaction was terminated by incubating it at 70°C for 5 minutes.

qRT-PCR reactions were conducted using a Step-One Plus RT-PCR thermal cycler (Applied Biosystems, USA) and SYBR Green qPCR Mix Reagent (Amplicon, Taiwan), in accordance with the manufacturer's instructions. Expressions of circ-PVT1 and circ-HIPK3 were normalized using *GAPDH*, as a reference gene, while expression of miR-25 and miR-149 was normalized using U6, as a reference gene. Each 20 µl reaction contained 10 µl of 2x Master Mix SYBR Green qPCR Mix Reagent (Amplicon, Taiwan), 0.5 µl of each primer (final concentration of 0.25 µM), 5 µl nuclease-free water and 4 µl cDNA. Nuclease-free water was included as a negative control in every qRT-PCR run to ensure that there was no contamination from non-template sources. We manually set the threshold value for all assays to determine the cycle threshold (Ct) value. The cycling conditions were as follows: an initial denaturation at 95°C for 20 seconds, followed by 40 cycles of 95°C for 5 seconds and 60°C for 30 seconds each. This was followed by a melting curve ranging from 60°C to 95°C, with fluorescence data being acquired every 0.3°C. To ensure specific amplification, we confirmed size of the amplicons by running them on a 2% agarose gel electrophoresis and analyzing the melting curve during the process. All reactions were performed in duplicate.

Statistical analysis

Statistical values are expressed as the mean ± SEM. The Shapiro-Wilk test was used to evaluate normality of the data distribution. Outliers were excluded from the analysis. Statistical analyses were conducted using GraphPad Prism 9.0 (GraphPad Software Inc.; San Diego, CA, USA). Multiple comparisons were analyzed using a single-factor ANOVA, followed by post-hoc comparisons using the Newman-Keuls test. A $P<0.05$ was considered statistically significant.

Results

Association of circ-HIPK3, circ-PVT1, miR-25, and miR-149 with radiation response

We aimed to analyze expression of circ-HIPK3, circ-PVT1, miR-25, and miR-149 in both radiosensitive and radioresistant BC cells, specifically MCF-7 and MDA-MB-231. We detected expression of circ-HIPK3, circ-PVT1, miR-25, and miR-149 in MCF-7 and MDA-MB-231 cells that were irradiated with 2Gy, 4Gy, and 8Gy X-rays using qRT-PCR.

We found that expression of circ-HIPK3 was significantly increased in MDA-MB-231 cells exposed to the dose of 8Gy for 48 hours, compared to the control group (expression ratio=18.16). The results of the non-parametric ANOVA test were statistically significant with $P<0.0001$.

A comparison of RNA expression between two cell lines showed a 72.64-fold increase of expression level in the MDA-MB-231 cell line compared to the MCF-7 cell line after 48 hours of exposure to the dose of 8Gy ($P<0.0001$). A comparison of circ-HIPK3 expression revealed a significant increase at radiation doses of 4Gy and 8Gy (14.76 and 6.01 times, respectively; $P<0.0001$ for both) in the MDA-MB-231 cell line after 48 hours (Fig.2A).

On the other hand, increases of circ-PVT1 expression level were observed in an MDA-MB-231 cell line at doses of 2Gy, 4Gy, and 8Gy after 24 and 48 hours, compared to the control. The expression ratios were 1.39, 1.61, 26.65, 1.23, 16.2, and 58.55, respectively. The results of the non-parametric ANOVA test were statistically significant with $P<0.0001$ for all of the tested variables. Moreover, a comparison between the two cell lines showed that after 24 hours of exposure to 8Gy radiation, and after 48 hours of exposure to 4Gy and 8Gy radiation, expression levels

of circ-PVT1 in the MDA-MB-231 cell line were 5.07, 7.3, and 9.5 times higher, respectively, than the MCF-7 cell line. The results of non-parametric ANOVA test were statistically significant with p-values of less than 0.0001 for the all three variables. In addition, expression level of circ-PVT1 was significantly higher in the MDA-MB-231 cell line after 24 hours exposure to radiation doses of 4Gy and 8Gy compared to 48 hours (10.56-fold and 2.19-fold, respectively). The results of non-parametric ANOVA test were statistically significant with p-values of less than 0.0001 for both variables (Fig.2B).

Furthermore, the expression of miR-25 in MDA-MB-231 cells was increased significantly at 24 and 48 hours post-exposure to 8Gy doses, with an expression ratio of 22.47 and 26.77, respectively, compared to the control group. The non-parametric ANOVA test results indicated statistical significance with p-values of less than 0.0001 for the both time-points. Findings showed that a dose of 8Gy increased miR-25 expression level by 449 and 535-fold in the MDA-MB-231 cell line, respectively, compared to the MCF-7 cell line after 24 and 48 hours (P<0.0001 for the both data, Fig.2C).

Moreover, an increase in miR-149 expression in the MCF-7 cell line was observed at dose of 8Gy after 24 and 48 hours, compared to the control. The expression ratios were 3.98, 3.98, and 5.86, respectively. The results of the non-parametric ANOVA test were statistically significant with P<0.0001 for all the tested variables.

Moreover, comparing the two cell lines at 8Gy demonstrated that expression level of miR-149 was 4.97 fold higher in the MCF-7 cell line after 24 hours and 6.51 fold higher after 48 hours, in contrast to the MDA-MB-231 cell line (P<0.0001 for the both data, Fig.2D).

Apoptotic rate

MCF-7 and MDA-MB-231 cells were cultured and then exposed to radiation. Morphological changes in the cells were observed under a light microscope (Fig.3). The data revealed that rate of apoptosis in the MCF-7 cell line was significantly higher in cells exposed to 4Gy and 8Gy compared to the control group after 24 hours (P=0.0002 and 0.0005, respectively). Results also showed that the cells receiving 8Gy had higher percentage of apoptotic cells compared to those receiving 2Gy and 4Gy at 24 hours. Additionally, the cells receiving 8Gy had higher percentage of apoptotic cells than those receiving control and 2Gy at 48 hours. It also showed a significant increase (P=0.016, P=0.032, P<0.0001 and P=0.01). The rate of cell apoptosis was significantly higher in the MCF-7 cell line, than the MDA-MB-231 cell line 24 hours after treatment with 8Gy radiation (P=0.007). The results also indicated that the MCF-7 cell line exhibited significantly higher levels of cell apoptosis compared to the MDA-MB-231 cell line after exposing to doses of 4Gy and 8Gy (P=0.013 and P=0.013, respectively, Fig.4).

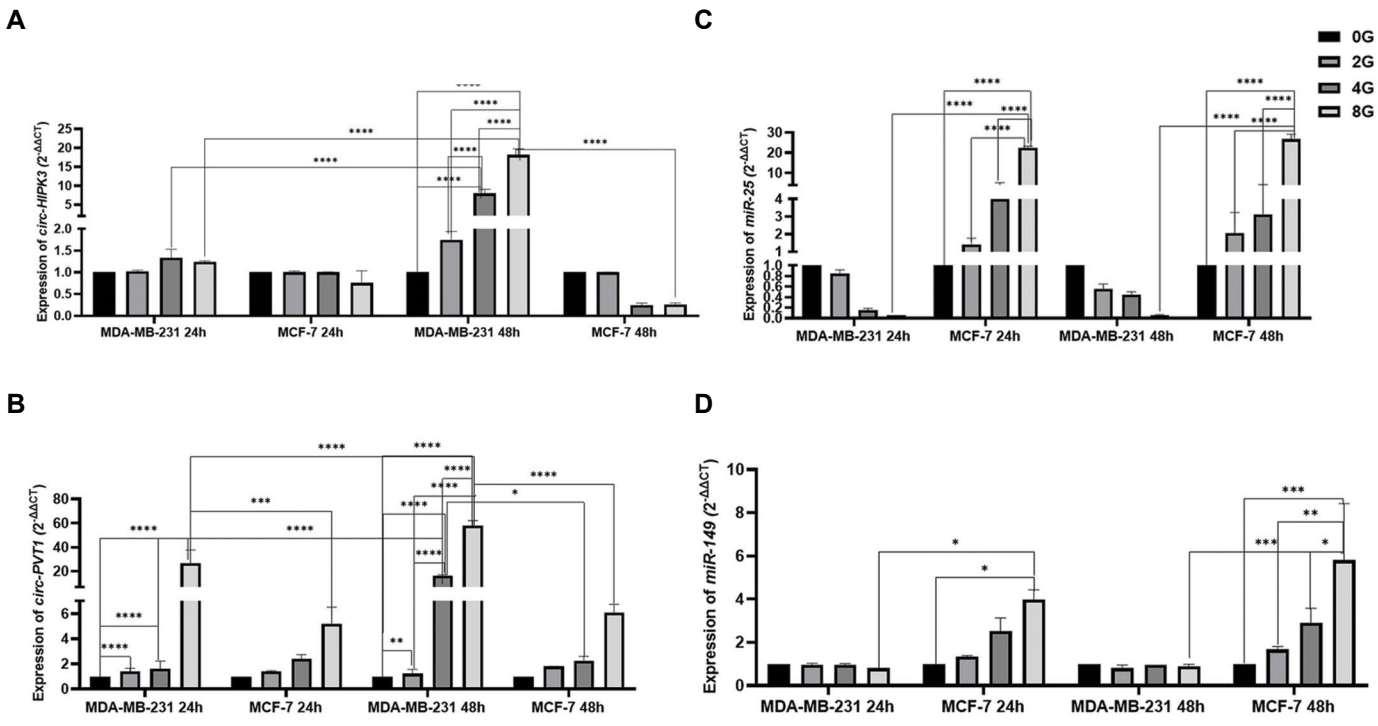

Fig.2: Comparison of the expression levels of RNAs in the control as well as irradiated MCF-7 and MDA-MB-231 cell lines (2Gy, 4Gy, and 8Gy) after 24- and 48 hours. **A.** circ-HIPK3, **B.** circ-PVT1, **C.** miR-25, and **D.** miR-149. The data was analyzed using Tukey's post-hoc one-way ANOVA. All experiments were performed three times. *; P<0.05, **; P<0.01, ***; P<0.001, and ****; P<0.0001.

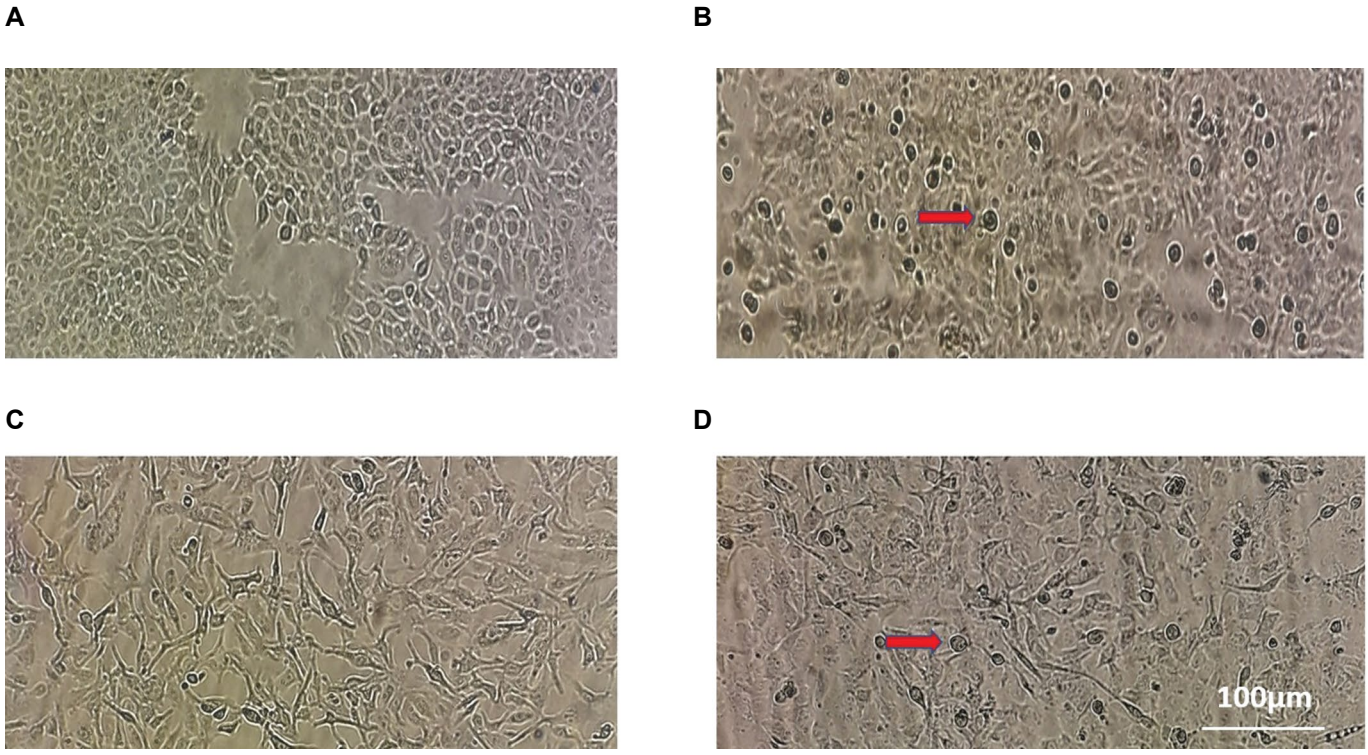

Fig.3: Morphological changes in cells observed under a light microscope. **A.** MCF-7 cells before irradiation. **B.** MCF-7 cells after irradiation. Apoptotic cells are indicated by red arrows. **C.** MDA-MB-231 cells before irradiation. **D.** MDA-MB-231 cells after irradiation. Apoptotic cells are indicated by red arrows. All experiments were performed three times (scale bar: 100 µm).

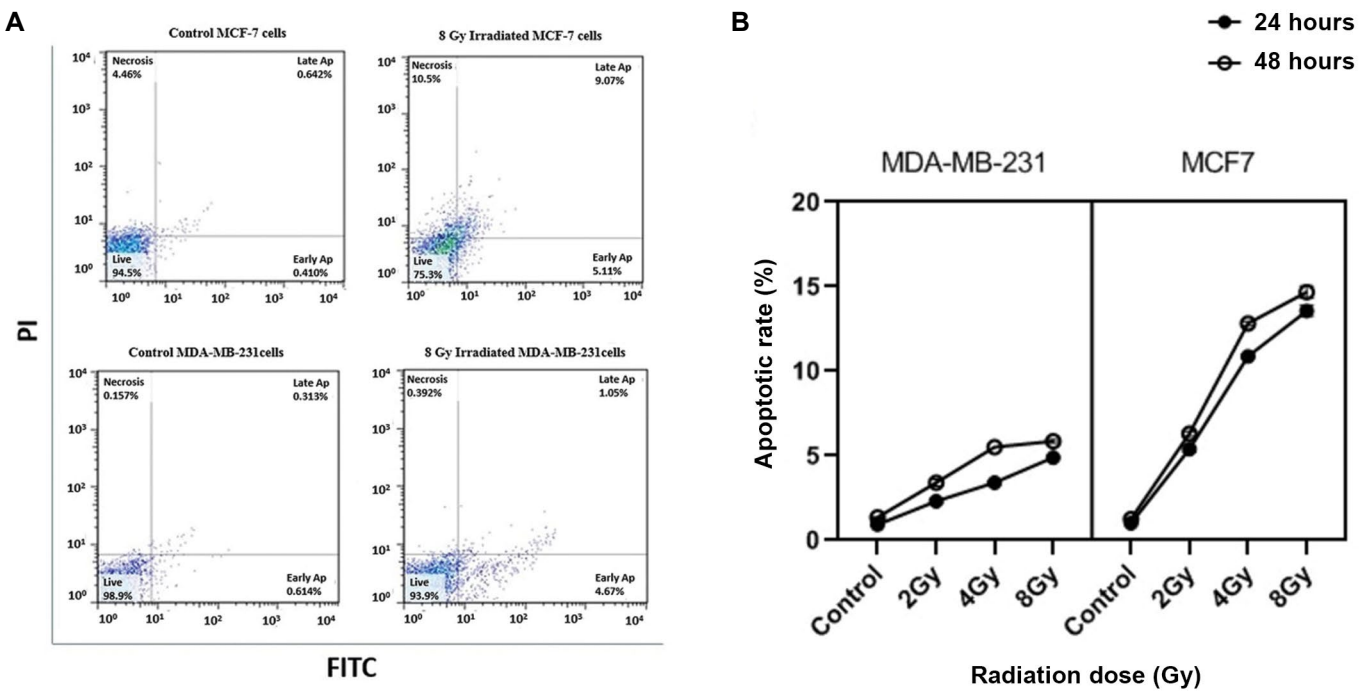

Fig.4: Flow cytometric analysis of apoptosis in cell lines. **A.** Detection of early and late apoptosis through flow cytometry assay using annexin V and PI staining. MCF-7 and MDA-MB-231 cells were exposed to 2, 4, and 8Gy of X-radiation for 24 and 48 hours, respectively. They were subsequently assessed using flow cytometry. MCF-7 cells were treated with medium alone as a control, without radiation. **B.** Rate of apoptosis in MCF-7 and MDA-MB-231 cells under radiation and control conditions. Data was analyzed using Tukey's post-hoc one-way ANOVA. All experiments were performed three times (scale bar: 100 µm).

Discussion

A potential avenue for radiosensitivity research involves developing risk models that incorporate genetic assays to predict a patient's response to radiation and the probability of experiencing radiation-induced side effects (26). This risk model can ultimately be combined with current predictors of radiosensitivity, such as radiation dose, developing the other diseases and conditions in addition to primary cancer, and volume of tissue exposed to radiation (27). The mechanism of RT involves directing X-rays at the affected area of body, which damages the double-stranded DNA. Healthy cells can repair this damage, while the cells with repair defects, such as cancer cells, undergo apoptosis and are eliminated. Previous studies have shown that rate of cell apoptosis was correlated with the level of radiation sensitivity (28). Moreover, cancer cells have high levels of reactive oxygen species (ROS) and they are selectively targeted for cell death by radiation. Degree of oxidative stress mediated by ROS is also linked to cellular radiosensitivity (29).

According to the results of this study, rate of cell apoptosis in the MCF-7 cell line following irradiation was significantly higher than the MDA-MB-231 cell line. This finding is consistent to the results obtained from another research (30).

Conducting the current study on additional cell lines would be beneficial to better establish role of radiation-sensitive or radiation-resistant RNAs. Additionally, conducting a functional study on the target proteins of these RNAs would provide more comprehensive understanding of their mechanisms. Unfortunately, limitations in this study prevented us from conducting such an investigation.

In the present study, we successfully demonstrated an increase in the expression levels of circ-HIPK3, circ-PVT1, and miR-25 in the MDA-MB-231 cell line, compared to the MCF-7 cell line after irradiation. Research indicated that circ-HIPK3, circ-PVT1, and miR-25 were highly expressed in specific types of malignancy, including BC (18, 19, 21). Previous studies demonstrated that circ-HIPK3 activated the NFκB/AKT pathway. Dysregulation of NFκB activity could cause alterations in the expression level of the genes regulated cell death, resulting in the upregulation of antiapoptotic and pro-survival genes, such as members of the Bcl-2 family, IAP proteins (XIAP, cIAP), and TNF receptor-associated factor (TRAF). Based on the previous studies which are in line with our findings, this dysregulation could also hinder apoptotic response to therapeutic agents (31, 32).

On the other hand, the previous studies showed that circ-PVT1 activated Arginase 2 (ARG2). This activation, in turn, inhibited BAX and activated bcl2, ultimately leading to inhibition of apoptosis (33). circ-PVT1 could regulate functions of PI3K/AKT, Wnt5a/Ror2, E2F2, and HIF-1α pathways. The AGR2-HIF-1α pathway, regulated by miR-29a-3p, was activated by circ-PVT1 in breast cancer, leading to increase of proliferation, invasion, and migration, while apoptosis was decreased. This suggested that circ-PVT1 functions as an oncogene in BC (34). Overexpression of circ-PVT1 enhanced expression of AGR2 and HIF-1α by inhibiting miR-29a-3p. During hypoxia, HIF-1α mediated an increase in Arg-II protein levels, which in turn increased production of mitochondrial ROS.

Another study showed that overexpressing miR-25 could decrease production of ROS and apoptosis in renal tubular epithelial cells by activating the PTEN/AKT pathway. These findings are consistent with the results of the current study (24, 35).

Furthermore, our findings demonstrated that expression of miR-149 was higher in the radiosensitive MCF-7 cell line compared to the MDA-MB-231 cell line. Additionally, the expression of miR-149 increased in parallel with higher rates of apoptosis. These results are consistent with the previous studies. Moreover, research studies demonstrated that miR-149 can efficiently inhibit migration and invasion of basal BC cells by targeting transcription factors SP1, FOXM1, and ZBTB2 (19). Previous studies revealed that overexpression of miR-149-5p led to reduction of the chaperonin TCP1 subunit 3 (CCT3) expression level. This reduction led to disruption of intracellular ROS homeostasis as well as redistribution of free amino acids for energy metabolism. This promoted apoptosis of tumor cells (36).

Conclusion

Our findings provided new evidence that circ-HIPK3, circ-PVT1, and miR-25 play crucial roles in the mechanisms of radioresistance in breast cancer. miR-149 was involved in cellular radiosensitivity and it may serve as a valuable factor for assessing cellular radiosensitivity *in vitro* for breast cancer. These factors could serve as a new therapeutic target for treatment of breast cancer. In future, additional studies should be conducted to investigate radiation sensitivity of patients with breast cancer. Establishing role of these factors as biomarkers for radiation sensitivity and resistance could provide valuable predictive information about tumor radiosensitivity or its response to treatment. This information could be used to personalize radiation dosing, making treatment more effective. This would enable clinicians to select from a variety of treatment options, while preventing radiation-induced toxicity in patients who are unlikely to benefit from the treatment.

Acknowledgments

This study was supported by the Tarbiat Modares University in Tehran, Iran, with a research ID: IG-39711. The authors sincerely appreciate the head and staff of the Oncology Department of Imam Khomeini Hospital for their valuable cooperation. The authors also thank all patients and healthy volunteers who participated in our study. We also thank H. Nosrati for irradiating the samples. There is no disclosed potential conflict of interest.

Authors' Contributions

E.A.; Collected samples, conducted experiments, analyzed data, and wrote the manuscript. H.M.; Designed and supervised the research plan, prepared and approved the final manuscript. All authors read and approved the final manuscript.

References

1. Jemal A, Bray F, Center MM, Ferlay J, Ward E, Forman D. Global cancer statistics. CA Cancer J Clin. 2011; 61(2): 69-90.
2. Delaney G, Jacob S, Featherstone C, Barton M. The role of radiotherapy in cancer treatment: estimating optimal utilization from a review of evidence-based clinical guidelines. Cancer. 2005; 104(6): 1129-1137.
3. Early Breast Cancer Trialists' Collaborative Group (EBCTCG); Darby S, McGale P, Correa C, Taylor C, Arriagada R, et al. Effect of radiotherapy after breast-conserving surgery on 10-year recurrence and 15-year breast cancer death: meta-analysis of individual patient data for 10,801 women in 17 randomised trials. Lancet. 2011; 378(9804): 1707-1716.
4. Liu X, Li F, Huang Q, Zhang Z, Zhou L, Deng Y, et al. Self-inflicted DNA double-strand breaks sustain tumorigenicity and stemness of cancer cells. Cell Res. 2017; 27(6): 764-783.
5. Jackson SP, Bartek J. The DNA-damage response in human biology and disease. Nature. 2009; 461(7267): 1071-1078.
6. Xu L, Lyu M, Yang S, Zhang J, Yu D. CircRNA expression profiles of breast cancer and construction of a circRNA-miRNA-mRNA network. Sci Rep. 2022; 12(1): 17765.
7. Zheng Q, Bao C, Guo W, Li S, Chen J, Chen B, et al. Circular RNA profiling reveals an abundant circHIPK3 that regulates cell growth by sponging multiple miRNAs. Nat Commun. 2016; 7: 11215.
8. Kong D, Shen D, Liu Z, Zhang J, Zhang J, Geng C. Circ_0008500 Knockdown improves radiosensitivity and inhibits tumorigenesis in breast cancer through the miR-758-3p/PFN2 axis. J Mammary Gland Biol Neoplasia. 2022; 27(1): 37-52.
9. Hu F, Peng Y, Fan X, Zhang X, Jin Z. Circular RNAs: implications of signaling pathways and bioinformatics in human cancer. Cancer Biol Med. 2023; 20(2): 104-128.
10. Zhang ZH, Wang Y, Zhang Y, Zheng SF, Feng T, Tian X, et al. The function and mechanisms of action of circular RNAs in urologic cancer. Mol Cancer. 2023; 22(1): 61.
11. Attwaters M. In vivo RNA base editing with circular RNAs. Nat Rev Genet. 2022; 23(4): 196-197.
12. He J, Xie Q, Xu H, Li J, Li Y. Circular RNAs and cancer. Cancer Lett. 2017; 396: 138-144.
13. Nielsen AF, Bindereif A, Bozzoni I, Hanan M, Hansen TB, Irimia M, et al. Best practice standards for circular RNA research. Nat Methods. 2022; 19(10): 1208-1220.
14. Zheng Q, Bao C, Guo W, Li S, Chen J, Chen B, et al. Circular RNA profiling reveals an abundant circHIPK3 that regulates cell growth by sponging multiple miRNAs. Nat Commun. 2016; 7: 11215.
15. Zeng K, Chen X, Xu M, Liu X, Hu X, Xu T, et al. CircHIPK3 promotes colorectal cancer growth and metastasis by sponging miR-7. Cell Death Dis. 2018; 9(4): 417.
16. Liu Z, Guo S, Sun H, Bai Y, Song Z, Liu X. Circular RNA CircHIPK3 elevates CCND2 expression and promotes cell proliferation and invasion through miR-124 in glioma. Front Genet. 2020; 11: 1013.
17. Chen D, Lu X, Yang F, Xing N. Circular RNA circHIPK3 promotes cell proliferation and invasion of prostate cancer by sponging miR-193a-3p and regulating MCL1 expression. Cancer Manag Res. 2019; 11: 1415-1423.
18. Zeng K, Chen X, Xu M, Liu X, Hu X, Xu T, et al. CircHIPK3 promotes colorectal cancer growth and metastasis by sponging miR-7. Cell Death Dis. 2018; 9(4): 417.
19. Lu H, Han X, Ren J, Ren K, Li Z, Sun Z. Circular RNA HIPK3 induces cell proliferation and inhibits apoptosis in non-small cell lung cancer through sponging miR-149. Cancer Biol Ther. 2020; 21(2): 113-121.
20. Luo N, Liu S, Li X, Hu Y, Zhang K. Circular RNA circHIPK3 promotes breast cancer progression via sponging MiR-326. Cell Cycle. 2021; 20(13): 1320-1333.
21. Ghafouri-Fard S, Khoshbakht T, Taheri M, Jamali E. A concise review on the role of CircPVT1 in tumorigenesis, drug sensitivity, and cancer prognosis. Front Oncol. 2021; 11: 762960.
22. Li M, Chi C, Zhou L, Chen Y, Tang X. Circular PVT1 regulates cell proliferation and invasion via miR-149-5p/FOXM1 axis in ovarian cancer. J Cancer. 2021; 12(2): 611-621.
23. Shi LP, Guo HL, Su YB, Zheng ZH, Liu JR, Lai SH. MicroRNA-149 sensitizes colorectal cancer to radiotherapy by downregulating human epididymis protein 4. Am J Cancer Res. 2018; 8(1): 30-38.
24. Zhao T, Meng W, Chin Y, Gao L, Yang X, Sun S, et al. Identification of miR253p as a tumor biomarker: regulation of cellular functions via TOB1 in breast cancer. Mol Med Rep. 2021; 23(6): 406.
25. He Z, Liu Y, Xiao B, Qian X. miR-25 modulates NSCLC cell radiosensitivity through directly inhibiting BTG2 expression. Biochem Biophys Res Commun. 2015; 457(3): 235-241.
26. Barnett GC, Wilkinson JS, Moody AM, Wilson CB, Twyman N, Wishart GC, et al. The Cambridge breast intensity-modulated radiotherapy trial: patient- and treatment-related factors that influence late toxicity. Clin Oncol (R Coll Radiol). 2011; 23(10): 662-673.
27. Tipatet KS, Davison-Gates L, Tewes TJ, Fiagbedzi EK, Elfick A, Neu B, et al. Detection of acquired radioresistance in breast cancer cell lines using Raman spectroscopy and machine learning. Analyst. 2021; 146(11): 3709-3716.
28. Dunne AL, Price ME, Mothersill C, McKeown SR, Robson T, Hirst DG. Relationship between clonogenic radiosensitivity, radiation-induced apoptosis and DNA damage/repair in human colon cancer cells. Br J Cancer. 2003; 89(12): 2277-2283.
29. Dayal R, Singh A, Pandey A, Mishra KP. Reactive oxygen species as mediator of tumor radiosensitivity. J Cancer Res Ther. 2014; 10(4): 811-818.
30. Wang W, Luo YP. MicroRNAs in breast cancer: oncogene and tumor suppressors with clinical potential. J Zhejiang Univ Sci B. 2015; 16(1): 18-31.
31. Li R, Wang X, Zhu C, Wang K. lncRNA PVT1: a novel oncogene in multiple cancers. Cell Mol Biol Lett. 2022; 27(1): 84.
32. Wang W, Nag SA, Zhang R. Targeting the NFκB signaling pathways for breast cancer prevention and therapy. Curr Med Chem. 2015; 22(2): 264-289.
33. Li R, Wang X, Zhu C, Wang K. lncRNA PVT1: a novel oncogene in multiple cancers. Cell Mol Biol Lett. 2022; 27(1): 84.
34. Wang J, Huang K, Shi L, Zhang Q, Zhang S. CircPVT1 promoted the progression of breast cancer by regulating MiR-29a-3p-mediated AGR2-HIF-1α pathway. Cancer Manag Res. 2020; 12: 11477-11490.
35. Li H, Zhu X, Zhang J, Shi J. MicroRNA-25 inhibits high glucose-induced apoptosis in renal tubular epithelial cells via PTEN/AKT pathway. Biomed Pharmacother. 2017; 96: 471-479.
36. Temiz E, Koyuncu İ, Sahin E. CCT3 suppression prompts apoptotic machinery through oxidative stress and energy deprivation in breast and prostate cancers. Free Radic Biol Med. 2021; 165: 88-99.